Do windbreaks reduce the water consumption of a crop field?

著者	SUGITA Michiaki
journal or publication title	Agricultural and Forest Meteorology
volume	250-251
page range	330-342
year	2018-03-15
権利	(C) 2017 Elsevier B.V.
URL	http://hdl.handle.net/2241/00151170

doi: 10.1016/j.agrformet.2017.11.033

Do windbreaks reduce the water consumption of a crop field?

Michiaki Sugita

Faculty of Life and Environmental Sciences, University of Tsukuba

---

Correspondence to: Michiaki Sugita, Faculty of Life and Environmental Sciences, University of Tsukuba, Tsukuba, Ibaraki 305-8572, Japan. E-mail: sugita@geoenv.tsukuba.ac.jp

Abstract

Two ratios, $A_c = \left[\frac{\left(q^*_c - q_a\right)\Big|_{u=\alpha u_0}}{\left(q^*_c - q_a\right)\Big|_{u=u_0}} \right] \Big/ \left[\frac{(r_c + r_{avc})\big|_{u=\alpha u_0}}{(r_c + r_{avc})\big|_{u=u_0}} \right]$ for the canopy layer and equivalent ratio A_g for the soil layer, were proposed for use to assess if soil evaporation (E_g) and canopy transpiration (E_c) decrease when wind speeds are reduced by windbreaks by a fraction of α, with q_a being the specific humidity of the air, q_c* the saturated specific humidity of the canopy layer, r_c the canopy resistance, and r_{avc} the aerodynamic resistance for moisture transfer. These ratios can be organized to form criteria, $\Delta E_c < 0$ ($A_c < 1$) and $\Delta E_g < 0$ ($A_g < 1$). Thus $\Delta E < 0$ if $A_c < 1$ and $A_g < 1$. If only one of the ratios is smaller than unity, the sign of ΔE depends on that of $\Delta E_g + \Delta E_c$. The criteria were examined by a dual-source crop community model to simulate energy and water balances of a crop field with data obtained in the Nile Delta. It was found that both $\Delta E \geq 0$ and $\Delta E < 0$ were possible and ΔE was mainly determined by ΔE_g during the fallow and early stages of the cropping seasons and by ΔE_c in the late cropping period. Overall, the scale of the roughness elements h_c and soil moisture θ were found to be the major factors to determine ΔE_c, ΔE_g, and ΔE. A larger h_c tends to produce $\Delta E \geq 0$; and ΔE_c and ΔE_g decrease as θ increases.

Keywords dual-source crop community model; maize; Nile Delta; evapotranspiration; soil evaporation; transpiration

1 Introduction

Effects of introducing windbreaks (WBs) on crop fields are one of the subjects that have drawn much interest in agricultural meteorology as well as in other disciplines (see, e.g., van Eimern et al. (1964) and Rosenberg (1979) for a review of earlier studies, and Cleugh (1998), Steven (1998), Cleugh (2002), Brandle et al. (2004) and Helfer et al. (2009) for a review on more recent works). This was because WBs have been expected to produce positive effects in a wide range of practical applications in agronomy. Evapotranspiration reduction has been one of them.

In spite of the long history of the WBs studies, however, we do not appear to have a full understanding of evapotranspiration differences caused by an introduction of WBs. For example, a review of Brandle et al. (2004) states that "Evaporation from bare soil is reduced in shelter… Evaporation from leaf surface is also reduced…" as if there is no exception. Campi et al. (2009, 2012) appear to be in this position. McNaughton (1988) and Cleugh (1998, 2002), on the other hand, mentioned that both decrease and increase of evapotranspiration were possible (see below in Section 2.3 for more details). In reality, there have been studies that reported increase (e.g., Baker et al., 1989), decrease (e.g., Miller et al, 1973; Campi et al., 2009, 2012), and both decrease and increase (e.g., Brown and Rosenberg, 1972; Cleugh, 2002) of evapotranspiration. This contradiction is perhaps not surprising because the influence of WBs on crop fields is quite complex.

McNaughton (1983) argued one such complexity of WBs that there are both direct and indirect effects on evapotranspiration of WBs. The direct effects arise from an altered turbulent exchange between the surface and the atmosphere. The indirect effects represent changes in evapotranspiration due to modified crop characteristics developed in different microclimates caused by WBs. Field studies based on measurements in a crop field with WBs often observe the combined effects of the direct and indirect effects. Theoretical approaches often focus on part(s) of such effects.

Thus the purposes of our study were (i) to revisit this problem of whether or not, evapotranspiration should decrease by the introduction of WBs; and (ii) to clarify major factors that cause the evapotranspiration differences due to WBs. In order to achieve these goals, first, we summarize available theories to study WBs influences, followed by the Methods section which introduces dual-source and single-source crop community models and dataset to be used in numerical experiments to simulate and compare energy and water balance with and without WBs. Finally, the Results and Discussion section list and discuss our findings. We focus our study on the direct influence of WBs on evapotranspiration, mainly based on the dual-source treatment of crop community. However, to facilitate comparison with previous studies, results from the single-source model are also presented. Also, in our experiments, the microclimate including temperature, humidity, and wind speeds in the internal boundary layer above the vegetated surface in the leeward of WBs is assumed given.

2 Theory

2.1 Influence of wind speeds reduction on a crop community

To study the influence of WBs, it was first assumed that a crop community consists of two layers, the canopy layer and the soil layer. Surface latent heat fluxes are expressed by the following bulk transfer equations (see, e.g., Brutsaert, 1982; Garratt, 1992)

$$
\begin{aligned}
L_e E_c &= \frac{\rho L_e \left(q_c * - q_a\right)}{(r_c + r_{avc})} \\
&= \frac{\rho c_p \left(e_c * - e_a\right)}{\gamma (r_c + r_{avc})}
\end{aligned}
\tag{1}
$$

for the canopy layer, and

$$L_eE_g = \frac{\rho L_e\left(q_g * - q_a\right)}{(r_g + r_{avg})} = \frac{\rho c_p\left(e_g * - e_a\right)}{\gamma(r_g + r_{avg})} \quad (2)$$

for the soil layer. L_e is the latent heat of vaporization; ρ is the atmospheric density; c_p is the specific heat of air at constant pressure; γ is the psychrometric constant; e_a and q_a are respectively the vapor pressure and specific humidity both in the air; and $e*$ and $q*$ are the saturated value of vapor pressure and specific humidity at single-source surface temperature. In Eqs. (1) – (2), and in the rest of this study, the subscript g and c represent the soil layer and canopy layer, respectively, and those without a subscript indicates the whole community. Thus E_g is the soil evaporation; E_c is the canopy transpiration; and E is the crop community evapotranspiration. r_c is the canopy resistance; r_g is the soil resistance; and r_{avc} and r_{avg} are the aerodynamic resistance for scalar transfer. Similarly, the sensible heat fluxes H_c and H_g are formulated by the following bulk equations (e.g., Brutsaert, 1982; Garratt, 1992)

$$H_c = \rho c_p C_{hc} u\left(T_c - T_a\right) \quad (3)$$

$$H_g = \rho c_p C_{hg} u\left(T_g - T_a\right) . \quad (4)$$

where C_h is the bulk transfer coefficient for sensible heat which is assumed to be the same as C_e, an equivalent coefficient for water vapor. T_a is the air temperature, T is the single-source surface temperature, and u is the wind speed.

When wind speed is reduced above each layer, the following reaction should take place according to Eqs. (1) and (2):

$$\left[u\downarrow\right]\rightarrow\left[r_{avc}\uparrow\right]\rightarrow\left[\frac{1}{(r_c+r_{avc})}\downarrow\right]\rightarrow\begin{bmatrix}E_c\downarrow\\H_c\downarrow\end{bmatrix} \tag{5}$$

and

$$\left[u\downarrow\right]\rightarrow\left[r_{avg}\uparrow\right]\rightarrow\left[\frac{1}{(r_s+r_{avg})}\downarrow\right]\rightarrow\begin{bmatrix}E_g\downarrow\\H_g\downarrow\end{bmatrix}. \tag{6}$$

An up or downward arrow beside each variable(s) indicates an increase or a decrease of the variable(s), respectively. From the 1st to the 2nd term of Eqs. (5) and (6), turbulence is weakened as shown by the increase of r_{avc} and r_{avg}, which should then reduce the turbulent exchanges of E_c, H_c, E_g, and H_g (3rd and 4th terms). However, the decrease of the outgoing fluxes (4th term) would induce an increase of source concentration, i.e., the single-source surface temperature T_c and T_g, as well as saturated specific humidity. These reactions can be summarized as follows:

$$
\begin{bmatrix} E_c \downarrow \\ H_c \downarrow \end{bmatrix} \rightarrow \begin{bmatrix} T_c \uparrow \\ q^*_c \uparrow \end{bmatrix} \rightarrow \begin{cases} \begin{bmatrix} (T_c - T_a) \uparrow \\ (q^*_c - q_a) \uparrow \end{bmatrix} \rightarrow \begin{bmatrix} E_c \uparrow \\ H_c \uparrow \end{bmatrix} \\ \left[\sigma T_c^4 \uparrow \right] \rightarrow \left[R_{nc} \downarrow \right] \rightarrow \begin{bmatrix} E_c \downarrow \\ H_c \downarrow \end{bmatrix} \end{cases} \tag{7}
$$

and

$$
\begin{bmatrix} E_g \downarrow \\ H_g \downarrow \end{bmatrix} \rightarrow \begin{bmatrix} T_g \uparrow \\ q^*_g \uparrow \end{bmatrix} \rightarrow \begin{cases} \begin{bmatrix} (T_g - T_a) \uparrow \\ (q^*_g - q_a) \uparrow \end{bmatrix} \rightarrow \begin{bmatrix} E_g \uparrow \\ H_g \uparrow \end{bmatrix} \\ \left[\sigma T_g^4 \uparrow \right] \rightarrow \left[R_{ng} \downarrow \right] \rightarrow \begin{bmatrix} E_g \downarrow \\ H_g \downarrow \end{bmatrix} \end{cases} \tag{8}
$$

where R_n is the net radiation; σ is the Stefan-Boltzmann constant; T is in K. From the 3rd term of Eqs. (7) and (8), there are two separate paths, one indicating increases of the gradients leading to the fluxes increases (negative feedback), and another showing a decrease of the net radiation, and the resulting decrease of H and E fluxes (positive feedback). Because there are feedback loops, an equilibrium should be reached (at least temporarily) for a given condition, somewhere in Eqs. (5) and (7), and Eqs. (6) and (8). The key variables that determine the equilibrium position are T_c and T_g because they link the bulk equations Eqs. (1) – (4) with energy balance equations of the crop community (see A.1.1. in the Appendix). Thus the equilibrium must be reached at the position where particular values of T_c and T_g satisfy all these equations simultaneously.

2.2 Criteria to determine the fate of evapotranspiration

In view of Eqs. (1) and (2), it is convenient to define the ratio A_c

$$A_c = \frac{E_c|_{u=\alpha u_0}}{E_c|_{u=u_0}} = \left.\frac{\left(q^*_c - q_a\right)}{(r_c + r_{avc})}\right|_{u=\alpha u_0} \Bigg/ \left.\frac{\left(q^*_c - q_a\right)}{(r_c + r_{avc})}\right|_{u=u_0}$$
$$= \left[\frac{\left(q^*_c - q_a\right)|_{u=\alpha u_0}}{\left(q^*_c - q_a\right)|_{u=u_0}}\right] \Bigg/ \left[\frac{(r_c + r_{avc})|_{u=\alpha u_0}}{(r_c + r_{avc})|_{u=u_0}}\right] \quad (9)$$

and the ratio A_g

$$A_g = \frac{E_g|_{u=\alpha u_0}}{E_g|_{u=u_0}} = \left.\frac{\left(q^*_g - q_a\right)}{(r_s + r_{avg})}\right|_{u=\alpha u_0} \Bigg/ \left.\frac{\left(q^*_g - q_a\right)}{(r_s + r_{avg})}\right|_{u=u_0}$$
$$= \left[\frac{\left(q^*_g - q_a\right)|_{u=\alpha u_0}}{\left(q^*_g - q_a\right)|_{u=u_0}}\right] \Bigg/ \left[\frac{(r_g + r_{avg})|_{u=\alpha u_0}}{(r_g + r_{avg})|_{u=u_0}}\right] \quad (10)$$

to argue the fate of E_g, E_c, and E when u becomes weaker from $u = u_0$ to $u = \alpha u_0$ ($0 \le \alpha < 1$). As is clear, whether WBs should reduce evapotranspiration can be judged by comparing the magnitude of the change in the gradient of the q concentration and that in resistances for the humidity transport. When the gradient change is larger ($A_c > 1$ or $A_g > 1$), the equilibrium is reached in the 2nd – 4th term in the upper path of Eqs. (7) – (8), and E_c and E_g should increase. Conversely, when the resistance change is larger (A_c

< 1 or A_g < 1), the equilibrium is likely reached in Eqs. (5) – (6) and E_c and E_g should decrease. Thus A_c and A_g can be organized to formulate the following criteria,

$$\Delta E_c \begin{Bmatrix} >0 & (A_c > 1) \\ =0 & (A_c = 1) \\ <0 & (A_c < 1) \end{Bmatrix}, \qquad (11)$$

$$\Delta E_g \begin{Bmatrix} >0 & (A_g > 1) \\ =0 & (A_g = 1) \\ <0 & (A_g < 1) \end{Bmatrix} \qquad (12)$$

and

$$\Delta E \begin{Bmatrix} >0 & \begin{pmatrix} \{(A_c>1)\wedge(A_g>1)\}\vee \\ \{(A_c<1)\wedge(A_g>1)\wedge(|\Delta E_c|<|\Delta E_g|)\}\vee \\ \{(A_c>1)\wedge(A_g<1)\wedge(|\Delta E_c|>|\Delta E_g|)\} \end{pmatrix} \\ =0 & \begin{pmatrix} \{(A_c=1)\wedge(A_g=1)\}\vee \\ \{(A_c<1)\wedge(A_g>1)\wedge(|\Delta E_c|=|\Delta E_g|)\}\vee \\ \{(A_c>1)\wedge(A_g<1)\wedge(|\Delta E_c|=|\Delta E_g|)\} \end{pmatrix} \\ <0 & \begin{pmatrix} \{(A_c<1)\wedge(A_g<1)\}\vee \\ \{(A_c<1)\wedge(A_g>1)\wedge(|\Delta E_c|>|\Delta E_g|)\}\vee \\ \{(A_c>1)\wedge(A_g<1)\wedge(|\Delta E_c|<|\Delta E_g|)\} \end{pmatrix} \end{Bmatrix} \qquad (13)$$

in which symbols $\wedge$ and $\vee$ represent the logical operation of "and" and "or" respectively. In our study, the Δx symbol represents the difference between x for $\alpha = 1.0$ and x for a specified value of α.

2.3 Analysis based on the Penman-Monteith equation

It is also possible to study ΔE in a simpler manner if one assumes a single-source model. McNaughton (1988) and Cleugh (1998, 2002) have introduced this approach by using the Penman-Monteith (P-M) equation given by

$$E_{PM} = \frac{1}{L_e}\left[\frac{s\left(R_n - G\right) + \rho c_p\left(e_a * - e_a\right)}{s + \gamma\left(1 + r_{c\_PM} / r_{a\_PM}\right)}\right] \tag{14}$$

where E_{PM} is the evapotranspiration; R_n is the net radiation; G the soil heat flux; s is the slope of the saturation vapor pressure (e_a*) curve at T_a; r_{a_PM} is the aerodynamic resistance; and r_{c_PM} is the surface resistance.

Whether evapotranspiration would be reduced when wind speed u was decreased can be studied by evaluating the sign of $\partial E_{PM} / \partial u$. It is convenient for this purpose to replace r_{a_PM} with

$$C_e u = 1/r_{av} = \frac{k^2}{\ln\left[\frac{z-d_0}{z_{0v}} - \Psi_v\left(\frac{z-d_0}{L}\right)\right]\ln\left[\frac{z-d_0}{z_0} - \Psi_m\left(\frac{z-d_0}{L}\right)\right]} \tag{15}$$

where z is the measurement height of u, T_a, and e_a; d_0 is the zero-plane displacement height; z_0 is the roughness length; z_{0v} is the scalar roughness for water vapor; Ψ is the stability correction function with the subscript v and m representing vapor and momentum transport (e.g., Brutsaert, 2005); and L is the Obukhov length. With a simple manipulation, it is possible to show

$$\frac{\partial E_{PM}}{\partial u}\begin{cases} >0 & \left(r_c > r_{c\_eq}\right) \\ =0 & \left(r_c = r_{c\_eq}\right) \\ <0 & \left(r_c < r_{c\_eq}\right) \end{cases} \tag{16}$$

where r_{c_eq} is the equilibrium canopy resistance defined by

$$r_{c\_eq} = \frac{\rho\left(q_a{*}-q_a\right)}{E_{eq}} \tag{17}$$

in which E_{eq} is the equilibrium evaporation.

$$E_{eq} = \frac{1}{L_e}\frac{s}{s+\gamma}\left(R_n - G\right). \tag{18}$$

As can be understood by referring to Eq. (17), r_{c_eq} is the canopy resistance that would be necessary to produce $E = E_{eq}$ under the actual dryness of the air ($q_a{*} - q_a$).

Note that McNaughton (1988) and Cleugh (1998) used different expressions from Eqs. (16) – (17). McNaughton (1988)'s version is

$$\frac{\partial E_{PM}}{\partial u}\begin{cases} >0 & \left((q_a^{*}-q_a) < D_{eq}\right) \\ =0 & \left((q_a^{*}-q_a) = D_{eq}\right) \\ <0 & \left((q_a^{*}-q_a) > D_{eq}\right) \end{cases} \tag{19}$$

and Cleugh (1998)'s version reads,

$$\frac{\partial E_{PM}}{\partial u}\begin{cases} >0 & \left(E_{eq} > E_{PM}\right) \\ =0 & \left(E_{eq} = E_{PM}\right) \\ <0 & \left(E_{eq} < E_{PM}\right) \end{cases} \tag{20}$$

in which $D_{eq} = E_{eq} r_{c\_PM} / \rho$. It is easy to show that Eqs. (16) - (17) can be converted into Eq. (19) or Eq. (20).

In our study, we mainly focus on the framework given in sections 2.1 – 2.2; however, to facilitate a comparison with previous studies, Eq. (16) will also be examined.

3 Methods

3.1 Dual-source crop community model

A dual-source crop community model was used to understand how soil evaporation E_g and transpiration E_c would respond to reduced wind speeds by means of WBs under given soil, vegetation, and meteorological conditions. The model consists of the canopy layer and the soil layer, and energy and water balance of the two layers were estimated.

The details of the model are explained in the Appendix. Briefly, those processes above the soil surface were formulated by means of three energy balance equations for the canopy layer, for the soil layer, and for the crop community; it was assumed that interactions between the atmosphere and the canopy layer, and those between the atmosphere and the soil surface work side by side, and the sum of the two fluxes results in the community level flux to satisfy the conservation equations (Kondo and Watanabe, 1992). Subsurface hydrological processes from the surface down to water table were also included in the model. They were formulated based on previous proposals with locally calibrated parameters whenever possible. Soil moisture content θ was then derived as the residual of the soil water balance equations and used to estimate the soil resistance r_{avg} and the canopy resistance r_{avc} which control E_g and E_c, respectively.

3.2 Dataset

A dataset obtained in an irrigated crop field without WBs in the Nile Delta in Egypt was used as inputs to the model. The details of the site, measurements, and experiments are explained in El-Kilani and Sugita (2017) and Sugita et al. (2017); briefly, the dataset was obtained in the Sakha-A field (31°5'54.7"N, 30°55'21"E) located in the central part of the Delta. An eddy correlation system together with meteorological and hydrological instruments was mounted on and around a 5-m tower at the center of a 200 by 200 m crop field (see Table 3 of Sugita et al. (2017) for the details of the measurements). In our analysis, those data obtained in the summer of 2011 were mainly used. The 2011 summer season consists of a fallow season (May 21 – June 13) and a summer cropping season (June 14 – September 17) in which maize (*Zea mays* L., cv., Three Ways Cross (Hybrid) 324) was cultivated using the furrow irrigation method with an irrigation interval of approximately two weeks. Other relevant variables of vegetation, soil, irrigation, etc. were also measured in this field.

3.3 Numerical experiments

3.3.1 Experiment I

In this experiment, nine sets of simulated outputs of energy and water balance components for a hypothetical crop field were generated for the 2011 summer season under various assumed conditions. El-Kilani and Sugita (2017) also produced six similar sets. In each set, simulations were carried out with wind speeds u specified as a fraction α of the measured wind speeds u_0 in the range of $0.1 \le \alpha \le 1.0$. For our study, three sets of outputs (run R1 – R3; Table 1), each with α =0.1, 0.9 and 1.0, were chosen out of these 15 sets so that the selected cases represent a wide variety of conditions and results of ΔE_c, ΔE_g, and ΔE .

Run R1 is the baseline case representing the maize field without WBs with the measured meteorological variables used as inputs. Run R2 represents the case in which T_a, q_a, and the soil surface roughness z_{0g} were altered from those of run R2. We varied z_{0g} to represent the surface condition of a different irrigation method. The z_{0g} value for the furrow irrigation is generally larger than that for a flat soil surface using drip and basin irrigation. By varying q_a, the case of altered microclimate in the so-called quiet and wake regions in the leeward of WBs can be realized. The magnitude of the q_a variation was determined from the observed differences between q_a in the leeward and in the windward of WBs in a field experiment in the Nile Delta (El-Kilani and Sugita, 2017). In the same experiment, the T_a differences were found negligible; nevertheless, we varied T_a in run R2 to see the influence of a different climatic condition.

The setting of run R3 is the same as that of run R1 except for the size of the crop, and the crop height (h_c) and leaf area index LAI (L_A) were altered from those of maize. The change of L_A is accompanied by that of the canopy transmittance f_c, the root zone depth z_{rz}, and the canopy cover fraction f_{cc}, while the change of h_c alters momentum and scalar roughness lengths (see Appendix).

3.3.2 Experiment II

This experiment was intended to focus specifically on the influence of the scale of roughness elements on ΔE, ΔE_c, and ΔE_g under the same condition as run R1 of experiment I. However, the simulations were carried out only for one day, August 1, selected arbitrarily from the midseason stage of maize. This was because meteorological conditions do not affect much in the outcome of ΔE, ΔE_c, and ΔE_g (see also the results presented in section 3.3) and that increased soil moisture to saturation did not produce markedly different simulated results for August 1, as was found in a preliminary analysis.

The same model was used except that the soil water balance part was disabled and water content value on this day determined in run R1 was prescribed as an input. The canopy height h_c was varied from the actual value of 2.2 m in the range of $0.1 < h_c /2.2 \leq 1.0$ at a 0.1 interval while other data were kept the same. L_A =2.6 (actual value on Aug.1) was adopted regardless of h_c in this experiment. The difference between the result for $\alpha = 0.1$ and those for 1.0 was examined.

4 Results and discussion

4.1 Different responses of the canopy and soil layers

Fig. 1a and b indicate the relation between ΔE and ΔE_c for the two cases of α = 0.1 and 0.9 based on the outputs of the experiment I. Clearly, both $\Delta E > 0$ and $\Delta E < 0$ occurred, which agree with McNaughton (1988) and Cleugh (1998, 2002), and assessments of observational studies mentioned in the Introduction section. It was found that $\Delta E > 0$ accounts for approximately 50 - 60%. A general positive correlation (R^2 = 0.83 - 0.85) can be noticed between ΔE_c and ΔE, if we ignore the points with $\Delta E_c = 0$ during the fallow season and other outlier points among the results of run R2 (α = 0.1) during the crop development stage when L_A and h_c were still small and soil surfaces were not fully covered by vegetation.

Fig. 1c and d show relationship between ΔE_c and ΔE_g. It is clear that there is essentially no correlation between ΔE_c and ΔE_g, and that there are many points with different signs of ΔE_c and ΔE_g. In the case of α = 0.9, the combination of $\Delta E_c > 0$ and

ΔE_g < 0 constitutes 32% while that of $\Delta E_c < 0$ and $\Delta E_g > 0$ accounts for 21%. In the case of α = 0.1, the percentages are 36% and 8%, respectively.

These results tend to imply that a single-source treatment of a crop community is likely an oversimplification if we need to study all stages of the cropping season. On the other hand, if the only target is the stages with mature canopy, it is likely acceptable to work with a single-source model.

Fig. 1e and f show whether the criterion given by Eq. (16) produced predictions of ΔE which agree with the ΔE results of the simulation runs. For this purpose, the outputs of runs R1, R2 and R3 of experiment I were organized accordingly and shown in Fig.1e for α=0.1, and in Fig.1f for α=0.9. The value of r_{c_PM} was determined by inverting Eq. (14) with the simulated values of E, R_n, G, and by setting $r_{a\_PM} = r_{av}$ in Eq. (17). It is immediately clear that there are cases which do not agree with what Eq. (16) suggests in both figures.

There should be at least four possible causes which induced failure of the criterion Eq. (16) to predict ΔE. First is the case when the sins of ΔE_c and ΔE_g were different. Failure is possible in this case because the canopy and the soil layers are treated together as a single layer in the P-M equation. These points are shown by brown open triangles or green squares symbols based on Eqs. (9) and (10). The majority of those points against Eq. (16) are found for $r_{c\_PM} / r_{c\_eq} < 1$ and $\Delta E > 0$, but some are for $r_{c\_PM} / r_{c\_eq} > 1$ and $\Delta E < 0$. The second cause is related to the fact that Eq. (16) is based on the derivative of the P-M equation evaluated at $u = u_0$ to estimate the change in *E* for an infinitely small change of *u* while ΔE was determined for a finite difference of $u = u_0$ and $u = \alpha u_0$; naturally they are not necessarily the same. The third cause originates from the fact that (16) does not consider the change in R_n resulting from the single-source surface temperature changes as indicated by Eqs. (7) and (8). Finally, the assumption in the derivation of the P-M equation, $s = \frac{de*}{dT_a} \approx \frac{e_s^* - e_a^*}{T_s - T_a}$, could be the source of disagreement. It is this assumption that allows us to use $\left(e_a^* - e_a\right)$, instead of the specific humidity difference between evaporating surface and the atmosphere $\left(q_s - q_a\right)$, as one of the driving forces of evapotranspiration.

4.2 Factors that influence ΔE_c, ΔE_g, and ΔE

Since surface fluxes are closely linked to the turbulent exchange between the surface and the atmosphere, the scale of the roughness elements is likely the first candidate to investigate as the main factor to determine ΔE_c, ΔE_g, and ΔE. This was studied with the results of experiment II (Fig. 2a – c).

Fig. 2a indicates that $\frac{\left(q^*_c - q_a\right)\big|_{u=0.1u_0}}{\left(q^*_c - q_a\right)\big|_{u=u_0}} > 1$ and $\frac{(r_c + r_{avc})\big|_{u=\alpha u_0}}{(r_c + r_{avc})\big|_{u=u_0}} > 1$ for all h_c values. This was caused by the increase of q^*_c and r_{avc} as u decreased and the turbulent exchange was suppressed (Eq. (5)). R_{nc} always decreased as u decreased (Eq. (7)).

It can also be noticed that $\frac{(r_c + r_{avc})\big|_{u=0.1u_0}}{(r_c + r_{avc})\big|_{u=u_0}}$ decreased while $\frac{\left(q^*_c - q_a\right)\big|_{u=0.1u_0}}{\left(q^*_c - q_a\right)\big|_{u=u_0}}$ increased when h_c increased. As a result, A_c kept increasing and became larger than 1.0 at h_c=1.93 m. This is where ΔE_c started to take positive values. Thus E_c tends to decrease when u is reduced for a smaller canopy while E_c increases are more likely to occur for a larger canopy. This is qualitatively in agreement with the assessment of Cleugh (1998) who showed, based on the P-M equation, the increase of the possibility of E reduction as the aerodynamic resistance increased (that is, as h_c decreased).

The fact that $\frac{(r_c + r_{avc})\big|_{u=0.1u_0}}{(r_c + r_{avc})\big|_{u=u_0}}$ decreased as h_c increased means that $(r_c + r_{avc})$ is more sensitive to the u change when the scale of the roughness elements is smaller. This can be understood by evaluating $\frac{\partial}{\partial u}(r_c + r_{avc}) = \frac{\partial}{\partial u}(1/C_h u) = -1/\left(C_h u^2\right)$ for a constant value of r_c. With a typical value of C_h = 0.004 for a small canopy (z_0 = 0.05m,

h_c = 0.2 m, d_0 = 2/3h_c, and z_{ov} = 6.8 10^{-3}), $\frac{\partial}{\partial u}(r_c + r_{avc}) = -42$ at u=2 m/s (z = 10 m/s).

For a large canopy, C_h = 0.006 (z_0 = 0.15 m, h_c = 2 m, d_0 = 2/3h_c, and z_{ov} = 2.0 10^{-2} m), and $\frac{\partial}{\partial u}(r_c + r_{avc}) = -63$ for the same wind speed. Therefore, $\frac{(r_c + r_{avc})|_{u=0.1u_0}}{(r_c + r_{avc})|_{u=u_0}}$ is 50% larger for the small canopy.

The same observations can be made for the soil layer (Fig. 2b) except that $A_g < 1$ and $\Delta E_g < 0$ all the time and their dependence on h_c is weak. As a result, the relation between ΔE and h_c is similar to that between ΔE_c and h_c except that $\Delta E < 0$ for all h_c values examined. Overall, it can be concluded that the size difference of the roughness elements affects mainly ΔE_c, and to a lesser degree ΔE_g.

3.3 Seasonal changes in ΔE_c, ΔE_g, and ΔE

In order to investigate how other factors than the roughness scale influence evapotranspiration differences due to WBs, a comparison was made between the simulated time series outputs for $u = u_0$ and those for $u = 0.1u_0$ during the summer season based on the results of experiment I (run R1).

Fig. 3a and b clearly show the same dependence of ΔE_c, ΔE_g, and ΔE on the roughness size observed in Fig. 2a - c: the canopy part is more sensitive to the roughness scale than the soil surface part; and $\frac{(r_c + r_{avc})|_{u=0.1u_0}}{(r_c + r_{avc})|_{u=u_0}}$ decreased, $\frac{\left(q^*_c - q_a\right)|_{u=0.1u_0}}{\left(q^*_c - q_a\right)|_{u=u_0}}$ increased, and A_c increased as h_c increased, particularly at later stages of the cropping season (after the middle of July). In this periods, $\Delta E_c \gg \Delta E_g$ and thus ΔE_c essentially controls the fate of ΔE. ΔE_c (and thus ΔE) shows a general decrease as h_c increased. However, these changes are not monotonous, unlike the case of Fig. 2a - c. For example, $\frac{(r_c + r_{avc})|_{u=0.1u_0}}{(r_c + r_{avc})|_{u=u_0}}$ shows periodic peaks in response to irrigation events. The same behavior can also be observed for $\frac{\left(q^*_c - q_a\right)|_{u=0.1u_0}}{\left(q^*_c - q_a\right)|_{u=u_0}}$. Those changes were caused by the increases in the θ value and resulting decreases in r_c and r_g. This agrees with Cleugh (1998) in general who indicated that wet soil conditions tended to result in the reduction of E. Also noticed in the figures are that the impact of irrigation was more pronounced in the early stages of the cropping season. This is because the root zone became deeper at later stages (Sugita et al., 2017) and therefore the soil moisture increase at an irrigation event became less pronounced.

In addition, it can be noted that in the fallow and early cropping seasons (through the middle of July), $\Delta E = \Delta E_g$ or $\Delta E \fallingdotseq \Delta E_g$ and thus behavior of ΔE_g is important. ΔE_g is mostly positive and shows periodic negative values. The cases of $\Delta E_g < 0$ correspond to the periods of increased θ with irrigation events. This is why $\Delta E_g > 0$ most of the time during the fallow season with small θ without irrigation events.

Seasonal changes in meteorological elements such as incoming radiation, air temperature, humidity and wind speed did not significantly affect ΔE_c, ΔE_g, and ΔE. This is partly because the climate in Egypt is stable (Sugita et al., 2017) and seasonal fluctuations in these elements were small during the cropping season. Therefore this part of the results could be area specific. Indeed, a comparison of the simulated results of different T_a and/or q_a values (results not shown) has indicated that the increased T_a and q_a tend to enhance the magnitude of ΔE_c and ΔE_g for $\alpha < 1$ while the increase of q_a alone weakened ΔE_c and ΔE_g.

Overall, factors which affected the seasonal changes in ΔE_c and ΔE_g can be summarized as the height of the roughness elements and surface resistance mainly controlled by soil moisture content.

5. Conclusions

In order to study the influence of windbreaks on crop evapotranspiration, two ratios (Eqs. (9) and (10)) have been proposed using the framework of a dual-source crop community model. They were organized to form the criteria given by Eqs. (11) - (13) to determine whether windbreaks could reduce evapotranspiration ($\Delta E < 0$).

It was shown that both $\Delta E > 0$ and $\Delta E < 0$ occurred in the results of the numerical experiments under three different conditions with two cases of wind speeds reduction by a fraction of $\alpha = 0.1$ and 0.9 using the dataset obtained in a crop field in the Nile Delta. The results with $\Delta E > 0$ account for approximately 50 - 60%. Generally, $\Delta E > 0$ can be observed as canopy height increased. This was because the main factor that determines ΔE_c and ΔE_g is the turbulent exchange which is influenced by the roughness scale. An additional contribution was made by the soil moisture increase due to irrigation events which reduce surface resistance for humidity transport above the soil and canopy layer. As a result, ΔE_c and ΔE_g decreased with θ increases. Meteorological factors of incoming radiation, air temperature, humidity, and wind speeds were found to have a minor influence in the case of the dataset obtained in the Nile Delta.

The results with different signs of ΔE_c and ΔE_g account for 42% ($\alpha = 0.1$) and 53% ($\alpha = 0.9$). In these cases, the sign of ΔE was determined mostly by ΔE_g during the fallow and early cropping seasons and by ΔE_c as the canopy height increased. The correlation between ΔE_c and ΔE_g was very weak. ΔE_c and ΔE, on the other hand, show a higher correlation in the later stages of cropping season with mature canopy. As a result, a single-source treatment of a crop community is not recommended to study windbreaks influences, particularly in the early stages of the cropping season when the soil surface plays an important role in the surface-atmosphere interaction; this can be treated better by the dual- or multi-layer crop community models. Indeed, the criterion (16) proposed based on the Penman-Monteith (P-M) equation did not always produce correct predictions of ΔE.

Acknowledgements

Authors are also grateful for El-Kilani, Rushdi M.M. (Cairo University) for participating field experiments and constructive discussion, for Fujimaki, H. (Tottori

University) and Hoshino, A. (Univ. Tsukuba) for providing us with their soil moisture and soil physics data, for Kubota, A. and Maruyama, S. (Univ. Tsukuba) for sharing their results on plant physiology and observation, for Fukuda, T., Matsuno A., Shimizu, T., Tsuchihira, K., Irigaki, Y. and Tsuji, I. (Univ. Tsukuba) for their participation in the field observations, and for Osada, A., Kamitani, T., Sayed El Nehlak, Hassan Mohamed Abd El Baki, and Hussein Al Nadar, among others (WAT project office, JICA) for supporting field observations for this study. Finally, the authors also express their appreciation to Satoh, M. (Univ. Tsukuba) without whose initiatives and leadership the experiment for this study would not have been possible. This research has been supported and financed, in part, through SATREPS of JST/JICA.

Appendix

A.1 Dual-source crop community model

A.1.1 Energy balance

The energy balance equation can be expressed as,

$$R_{nc} = (1-f_c)\left(R_{sd} - R_{su} + R_{ld}\right) + (1-f_c)\sigma T_g^{\,4} - 2(1-f_c)\sigma T_c^{\,4} = H_c + L_e E_c \quad \text{(A.1)}$$

for the canopy layer, as

$$R_{ng} = f_c\left(R_{sd} - R_{su} + R_{ld}\right) + (1-f_c)\sigma T_c^{\,4} - \sigma T_g^{\,4} = H_g + L_e E_g + G \qquad \text{(A.2)}$$

for the soil layer, and as

$$R_n = \left(R_{sd} - R_{su} + R_{ld}\right) - \left[f_c \sigma T_g^{\,4} + (1-f_c)\sigma T_c^{\,4}\right] = H_g + L_e E_g + H_c + L_e E_c + G \quad \text{(A.3)}$$

for the crop community. In Eqs. (A.1) – (A.3), R_{sd} and R_{su} are the downward and upward short-wave radiation; R_{ld} is the downward long-wave radiation; f_c is the canopy transmissivity; and G is the soil heat flux.

A.1.1.1 Resistance parameterizations

The soil resistance r_g was estimated by

$$r_g = \frac{a_1(\theta_s - \theta)^{b_1}}{D_0\left(\dfrac{T_g}{273.16}\right)^{1.75}} \qquad \text{(A.4)}$$

(Kondo et al., 1990) where $D_0 = 2.23\times10^{-5}$ m^2/s is the molecular diffusivity at soil surface temperature T_g = 0°C, and a_1 and b_1 are the soil-type specific constants. Model calibration with the data during the fallow period allowed determination of these constants (see section A.3 and Table A.1).

The canopy resistance r_c was estimated based on the so-called Jarvis-type models (e.g., Jacquemin and Noilhan, 1990),

$$r_c = r_{st,\min} / \left(L_A f_1 \left(R_{sd} \right) f_2 \left(e_a^* - e_a \right) f_3 \left(T_a \right) f_4 \left(\theta \right) \right) \tag{A.5}$$

where $r_{st,min}$ is the minimum bulk stomatal resistance, f_1 through f_4 ($0 \le f \le 1$) are respectively a function of R_{sd}, that of ($e_a^* - e_a$), and so on. The same functional forms of Jacquemin and Noihen (1990) were adopted, but the coefficients were determined by the resistance measurements of maize in the Sakha-A field (Kubota, 2014, personal comm.). They are,

$$f_1 = \left(F + \frac{r_{st,\min}}{r_{st,\max}} \right) \frac{1}{1+F} \tag{A.6}$$

where $r_{st,max}$ is the maximum bulk stomatal resistance and F is another function

$$F = \left(0.55 \frac{R_{sd}}{R_{gl}} \frac{1}{L_A} \right) \tag{A.7}$$

and

$$f_2 = \begin{cases} 0.1 & \left\{ \left(e_a^* - e_a \right) \ge 10 \text{ hPa} \right\} \\ \left[1 - a_2 \left(e_a^* - e_a \right) \right]^{b_2} & \left\{ \left(e_a^* - e_a \right) < 10 \text{ hPa} \right\} \end{cases} \tag{A.8}$$

The value of $r_{st,\,min}$ was also adopted initially from the in situ measurements by Kubota (2014, personal comm.), but in the calibration stage, it was adjusted to produce the best agreement between the measured E and the simulated E values, on average, during the cropping season of maize, after the parameters of r_g had been calibrated (see section A.3). The final value together with coefficients a_2 and b_2 are listed in Table A.1. Other functions are

$$f_3 = 1 - a_3\left(T_{a,ref} - T_a\right)^2 \tag{A.9}$$

where a_3 = 0.0016 (Jacquemin and Noihan, 1990) is a coefficient, and $T_{a,ref}$ is the air temperature that produces the smallest r_{st}, and

$$f_4 = \frac{\theta - \theta_w}{\theta_{fc} - \theta_w} \ . \tag{A.10}$$

in which θ_w is θ at the wilting point and θ_{fc} is the field capacity.

The values of r_{ac} and r_{ag} were determined from Eq. (15) and the equivalent equation for the soil layer from bulk transfer coefficients (see below in section A.1.1.2).

A.1.1.2 Bulk transfer coefficients

The bulk transfer coefficients of the maize community for sensible heat C_h were determined from Eq. (15) for each time step with momentum roughness z_0 and scalar roughness z_{0h} by assuming similarity between the sensible heat and latent heat transport. Similarly, the bulk transfer coefficients at soil surface C_{hg} were determined from z_{0g} and

z_{0hg}. Finally, the bulk transfer coefficients for the canopy layer C_{hc} were determined from

$$C_{hc} = C_h - C_{hg} . \qquad \text{(A.11)}$$

The momentum roughness of the soil surface z_{0g} was determined by applying the method of Toda and Sugita (2003) in which the z_{0g} value was selected, that produced the best agreement of friction velocity u_* values estimated from the profile equation in the surface layer,

$$u(z) = \frac{u_*}{k}\left[\ln\left(\frac{z-d_0}{z_0}\right) - \Psi_m\left(\frac{z-d_0}{L}\right)\right] \qquad \text{(A.12)}$$

and those measured by the eddy correlation method (Sugita et al., 2017). The application was made to the data during the fallow season when d_0=0 and z_0 =z_{0g}. The selected z_{0g} value (Table A.1) is larger than the textbook value for bare soil surfaces. This is reasonable as the Sakha-A field was cultivated using furrow irrigation (the bed interval: 0.8 m, and the bed width and height: 0.2 m each). The larger z_{0g} obviously reflects this rougher surface condition.

The scalar roughness length of the soil surface z_{0hg} was also determined by the same procedure. However, instead of u_* values, the sensible heat fluxes H were compared to select the optimum z_{0hg} value. Corresponding profile equation for H reads,

$$T_g - T_a(z) = \frac{H}{ku_*\rho c_p}\left[\ln\left(\frac{z-d_0}{z_{0h}}\right) - \Psi_h\left(\frac{z-d_0}{L}\right)\right] \qquad \text{(A.13)}$$

and in the analysis, $d_0 = 0$ and $z_{0h} = z_{0hg}$ were assigned.

Also determined were the momentum roughness z_0 and the scalar roughness for sensible heat z_{0h} of the crop community. The determination was made several times during the maize cropping season by applying the same procedure outlined above. The following regression equations were derived that relate canopy height h_c with z_0 and z_{0h}

$$z_0 = 0.0292 + 0.000828h_c - 0.00573h_c^2 + 0.0135h_c^3 \qquad \text{(A.14)}$$

$$z_{0h} = \exp\left(-6.76 - 0.284h_c + 0.677h_c^2\right)$$

from which daily values were estimated.

A.1.1.3 Wind speeds below canopy

For the application of Eqs. (2) and (4), the wind speeds below canopy at $z = z_g$ were estimated from the measured wind speeds above the canopy. $z_g = 0.1$ m was arbitrarily selected. First, $u(h_c)$ was estimated from the measurement at $z = 5.78$ m by applying the wind profile equation Eq. (A.12). Then the wind profile function below canopy (Inoue, 1963),

$$u(z_g) = u(h_c)\exp\left[-a_4\left(1 - z_g / h_c\right)\right] \quad \text{(A.15)}$$

was applied to $u(h_c)$ for the case of $h_c > 0.1$ m, with the coefficient $a_4 = 2.0$ based on Inoue and Uchijima (1979). The estimated $u(z_g)$ was finally converted to u at $z = 5.78$ m by applying (A.12) for use in the model. When $h_c \leq 0.1$ m, the measured u at $z = 5.78$ m was simply used in the model by ignoring the small canopy.

Note that wind profile functions such as (A.15) have been developed from the horizontal equation of motion in the absence of a pressure gradient and the Coriolis force but with a momentum sink term due to the presence of stems and leaves below a canopy. Assumptions were then made that the shear stress is proportional to the wind speed gradients by means of eddy viscosity K_m and that the sink term is proportional to u(z), the foliage drag coefficient cd_f and the foliage surface area A_f. (A.15) can be obtained if we assume of a constant value of $A_f\, cd_f$ and a constant mixing length (and thus K_m). Other functions can be obtained by assuming a different form of K_m (e.g., Cowan, 1968). Also, adopting different closure scheme other than the mixing length approach allows derivation of different forms (e.g., Yi, 2008); however, this approach is not without criticism (Finnigan et al, 2015). Massman et al. (2017) adopted a parameterization of $u_*/u(h_c)$ as a function of height and proposed a wind profile model which is a combination of two functions, one mainly representing the upper part of wind profile and another near the surface. It was aimed to represent a realistic wind profile near the surface, which should be close to a logarithmic shape with $u(z)$ approaching zero at z_0.

Although it was tempting to use the model by Massman et al. (2017) as it likely produces a more realistic value of $u(z_g)$ near the surface, it was decided not to adopt this model at present since it was tested only by one profile measurement for maize. In contrast, (A.15) has been tested and used extensively and successfully in the literature. However, to test uncertainties to use (A.15), $u(z_g)$ values from (A.15) were changed by ±15% in the numerical experiments, and the results were compared against those from simulations without change of $u(z_g)$. The conclusions obtained in our study with (A.15) were found to remain the same with ±15% changes of $u(z_g)$ values.

A.1.1.4 Canopy transmittance and coverage

The canopy transmittance f_c and LAI (L_A) were determined by a canopy analyzer (Li-cor, LAI2200 or LAI2000) several times during the maize cropping season at multiple locations in the field (Fukuda, 2012; Tsuchihira, 2011); the measurements were made around noon for the f_c measurement, and shortly after sunset for L_A. These data were used to determine the following empirical equation

$$f_c = 1 - 1.015\left[1 - \exp\left(-0.633 L_A\right)\right] \tag{A.16}$$

which was used to estimate the daily value of f_c as a function of L_A in the model.

The canopy cover fraction f_{cc} was necessary to estimate infiltration of rainfall differently under the canopy and in the canopy gaps. However, no rainfall was recorded during the 2011 summer season, and f_{cc} was therefore not used for our study. Nevertheless, for the sake of completeness, the empirical function adopted in the model is given below as

$$f_{cc} = 34.097 L_A^{\;0.551}. \tag{A.17}$$

in which its functional form and coefficients were determined by comparing the measured L_A and f_{cc} values. The values of f_{cc} were determined by image processing of digital camera images taken at a nadir-looking position at eight locations in the field (Tsuchihira, 2011; see also Byambakhuu et al, 2010 for the details of the method).

A.1.2 Water balance

The water balance equations for the crop community including the soil layer beneath the surface are given by

$$\frac{dS_w}{dt} = -\frac{dS_s}{dt} + I_g + W_{rz} - I_{rz} - E_c \quad \text{(A.18)}$$

$$\frac{dS_s}{dt} = P_i + P_r - I_g - E_g \quad \text{(A.19)}$$

in which P_i is the irrigation, P_r is the rainfall, S_s is the surface water storage resulting from P_i or P_r, I_g is the infiltration into the soil at soil surface, I_{rz} is the drainage from the bottom of the root zone $z = z_{rz}$, W_{rz} is the upward capillary flux evaluated at z_{rz}, and S_w is the water storage in the form of soil moisture in the soil layer. Also, the community level evapotranspiration is given by

$$E = E_g + E_c. \quad \text{(A.20)}$$

The thickness of the soil layer was arbitrarily determined as 0.17 m for the fallow season and set equal to the depth of the root zone (z_{rz}) during the cropping season which was given as a function of L_A (see below in section A.1.2.3).

Soil water content was estimated as a residual of Eq. (A.18) – (A.19) by considering two cases. The first case was when the top of the capillary fringe on water table was within the soil layer. In this case, saturation was simply assumed in the soil layer. The second case was when the top of the capillary fringe was below the soil layer. Then, the mean θ in the soil layer was estimated in the model by solving soil water balance Eq. (A.18) for S_w. To determine which case applies, the depth to water table (z_{gw}) was used. The depth of the capillary rise was assumed constant at air entry value (Hb) (see Table A.1).

A.1.2.1 Depth to water table

Groundwater level was measured continuously in an observation well of a depth of 2 m. The timing and amount of the irrigation were also recorded (Sugita et al., 2017). They were used to derive the relation between z_{gw} and the elapsed time t (d) measured from the end of the last irrigation event. It was found that the relationships observed in different events looked similar, and therefore it was decided to estimate z_{gw} in meters by the following empirical function fitted to the measurements,

$$z_{gw} = 1.1\left[1 - \exp\left(-\left\{(t - 0.115)/2\right\}^5\right)\right]. \quad \text{(A.21)}$$

A.1.2.2 Soil water balance components

In Eq. (A.19), P_r can be neglected for the present purpose to apply the model in the Nile Delta where rainfall during summer is usually zero. The surface storage S_s at an *i*-th time step was determined from $S(i) = S(i-1) + \left[P_i(i-1) - I_g(i-1) \right] \Delta t$ in which Δt is the time step employed for the model implementation (=1 d). The infiltration into the soil at surface I_g was estimated from the following expression of Milly (1986),

$$I_g = a_5 \left\{ 1 + \left[-1 + \left(1 + \frac{4a_5 i_{gc}}{A_0^2} \right)^{0.5} \right]^{-1} \right\} \tag{A.22}$$

which makes use of the infiltration capacity (Philip, 1957). In Eq. (A.22), a_5 is a constant and assumed as 1/2 of the hydraulic conductivity K_s (Table A.1); A_0 is the sorptivity and was estimated from

$$A_0 = 1.458 \theta_u^{\ 0.165} \left[\int_{-\infty}^{0} \theta^{0.67} K_s d\psi \right]^{1/2} \tag{A.23}$$

(Eq. (11) of Milly (1986)), in which ψ is the matric head, and θ_u is θ at satiation with ψ =0 (Table A.1). The values of A_0 for different depth ranges of the root zone were calculated by Eq. (A.23) and are listed in Table A.1). i_{gc} is the cumulative infiltration (Philip, 1957) given by

$$i_{gc} = A_0 \tau^{-1/2} + a_5 \tag{A.24}$$

in which τ is the elapsed time measured from the start of the irrigation event.

Parameters in these equations (Table A.1) were derived from soil samples taken in the Sakha-A field and subsequent laboratory experiments (Fujimaki and Hoshino, 2010, Personal comm.).

The drainage I_{rz} from the bottom of the root zone $z = z_{rz}$ was determined by

$$I_{rz} = K(\theta_{rz}) \tag{A.25}$$

in which $K(\ )$ is the unsaturated hydraulic conductivity as a function of soil water content θ at z_{rz}. The $K(\ )$ values of soil samples taken in the Sakha-A field were determined by Fujimaki and Hoshino (2010, Personal comm.). The parameter a_6 (Table S.1) of the following expression by Brooks and Corey (1966) was determined by fitting Eq. (A.26) to the data,

$$K(\theta) = K_s \left(\frac{\theta}{\theta_s} \right)^{(2+3a_6)/a_6} . \tag{A.26}$$

The upward capillary flux W_{rz} was set equal to zero because soil water potential measurements at two levels (−0.7 and −0.9 m) above water table indicated steady downward moisture flux (Fujimaki, personal comm., 2013).

A.1.2.3 Root zone depth

The depth of the root zone was determined from root distribution measurements of Tsuchihira (2011), and additionally from the data of Fujimaki (2014, personal comm.). Tsuchihira (2011) measured the dry weight of all root systems in a soil block of 0.2×0.2×0.1 m taken from the surface to −0.5 m at a 0.1-m interval. For our study, the following functional relationships were established for the maximum depth z_{rz} obtained for maize using the drip irrigation and using the furrow irrigation.

$$z_{rz} = \begin{cases} 0.483\exp\left(-L_A / 1.092\right) - 0.49 & \text{(furrow)} \\ 0.550\exp\left(-L_A / 0.352\right) - 0.56 & \text{(drip)} \end{cases} . \tag{A.27}$$

In the case of $z_{rz} < 0.1$ m, $z_{rz} = 0.17$ m was arbitrarily assigned.

A.2 Model implementation

The simulation was carried out starting on April 1 in experiment I, to provide a spin-up period for the model to produce reasonable soil moisture at the beginning of the summer season on May 21.

The model was solved for each time step by employing an iteration procedure. More specifically, initial guess values of T_g and T_c were assigned and this allowed initial estimations of H_g, E_g, H_c, and E_c from Eqs. (1) - (4), which were then inserted into the right-hand side of Eqs. (A.1) – (A.3) and Eqs. (A.18) – (A.19) to examine whether or not the energy balance of each layer closed sufficiently. If the closure was not satisfactory, T_g and T_c were adjusted and the results were again examined for the energy balance closure; this process was repeated until the closure had been achieved sufficiently (<5 W/m^2) for both (A.1) and (A.2).

The model was operated at a daily time step. The atmospheric stability was considered. This was because evapotranspiration takes place mainly during daytime under unstable atmospheric conditions, and even if daily averaging was employed, resulting daily mean fluxes of H, E and u_* usually indicate unstable conditions. Therefore the daily values of the Obukhov length L were determined from the measured daily mean values of H, L_eE and u_* and were used in all simulation runs. Note that a more accurate treatment should have been an iteration procedure, in which the first H and L_eE values produced by the model, and u_* obtainable from the wind speed data and the profile equation Eq. (A.12) with assumed neutral stability, can be used to derive the first estimate of L, which in turn allows the second estimate of the fluxes, and so on. However, this is quite complicated and was not adopted because the stability correction functions Ψs are only a mild function of z/L.

A preliminary analysis carried out to compare the results from hourly simulation and those from daily simulation did not show significant differences so that the implementation of the model at a daily time step with the stability effect was judged acceptable for the present purpose.

A.3 Model calibration

The estimated values of E and E_g were compared with the measurements in order to calibrate the coefficients in Eqs (A.4) and (A.5). As mentioned above, it was aimed to produce the best agreement between the measured E and the simulated E values, on average. A regression constant a = 1.00, the coefficient of determination R^2 = 0.94 for a regression equation through the origin $\hat{y} = ax$ (x and y represent the simulated and the measured variables), and the RMS difference = 0.51 mm (defined as $\left[\sum (x_i - y_i)^2 / n\right]^{0.5}$) were obtained for the fallow season; similarly, a = 0.99, R^2 = 0.97, and the RMS difference = 0.70 mm were obtained for the cropping season. On average, the model reproduced E values (or E_g during the fallow season) reasonably well (see also Fig. A.1.

A comparison was also made visually between the measured and the simulated time series variables of E, θ, and R_{lu}, the upward long wave radiation (Fig. A.2). Although the time changes in all three variables are well reproduced by the model, the agreement in terms of magnitude is not necessarily excellent, particularly for θ. However, as can be seen from the comparison of the E time series, the errors in θ did not propagate into the evapotranspiration estimation too much. This was partly because the errors in θ were absorbed into r_g through a model calibration as explained above.

References

Baker, G.L., Hatfield, J.L., Wanjura, D.F., 1989. Influence of wind on cotton growth and yield. Trans. ASAE, 32, 97-104.

Brandle, J.R., Hodges, L., Zhou, X.H., 2004. Windbreaks in North American agricultural systems. Agrofor. Syst., 61, 65-78.

Brooks, R.H., Corey, A.T., 1966. Properties of porous media affecting fluid flow. Proc. Am. Soc. Civ. Eng., J. Irrigation Drainage Div. IR2, 61-68.

Brown, K.W., Rosenberg, N.J., 1972. Shelter-effects on microclimate, growth and water use by irrigated sugar beets in the great plains. Agr. Meteorol., 9, 241-263.

Brutsaert, W., 1982. Evaporation into the Atmosphere: Theory, History, and Applications. D. Reidel Pub. Co., Dordrecht.

Brutsaert, W., 2005. Hydrology: An Introduction. Cambridge University Press, Cambridge.

Byambakhuu, I., Sugita, M., Matsushima, D., 2010. Spectral unmixing model to assess land cover fractions in Mongolian steppe regions. Remote Sens. Environ., 114, 2361-2372. doi:10.1016/j.rse.2010.05.013.

Campi, P., Palumbo, A.D., Mastrorilli, M., 2009. Effects of tree windbreak on microclimate and what productivity in a Mediterranean environment, Eur. J. Agron., 30, 220-227. doi:10.1016/j.eja.2008.10.004

Campi, P., Palumbo, A.D., Mastrorilli, M., 2012. Evapotranspiration estimation of crops protected by windbreak in a Mediterranean region. Agri. Wat. Manage, 104,153–162, doi:10.1016/j.agwat.2011.12.010

Cleugh, H.A., 1998. Effects of windbreaks on airflow, microclimates and crop yields. Agroforestry Systems, 41, 55-84.

Cleugh H.A., 2002. Parameterising the impact of shelter on crop microclimates and evaporation fluxes. Australian J. Exp. Agricul., 42, 859-874.

Cowan, I.R., 1968. Mass, heat and momentum exchange between stands of plants and their atmospheric environment. Q. J. R. Meteorol. Soc. 94, 523-544, doi: 10.1002/qj.49709440208

El-Kilani, R.M.M. and Sugita, M., 2017. Irrigation methods and water requirements in the Nile Delta. In*:* M. Satoh and S. Aboulroos, eds. Irrigated Agriculture in Egypt-Past, Present and Future*.* Springer, 125-151, doi: 10.1007/978-3-319-30216-4_6

Finnigan, J.J., Harman. I.N., Ross, A.N., Belcher, S.E., 2015. First order turbulence closure for modelling complex canopy flows. Q. J. R. Meteorol. Soc. 141, 2907–2916, doi:10.1002/qj.2577

Fukuda, T., 2012. Estimation of evapotranspiration in agricultural land of the Nile Delta and verification of effect of evaporation control measures: A case of maize in summer. MS Thesis, Graduate School of Life and Environmental Science, University of Tsukuba. (in Japanese)

Garratt, J., 1992. The Atmospheric Boundary Layer. Cambridge University Press, Cambridge.

Helfer, F., Zhang, H., Lemckert, C., 2009. Evaporation Reduction by Windbreaks: Overview, Modelling and Efficiency. Urban Water Security Research Alliance Technical Report, No.16, 18p.

Inoue, E., 1963. On the turbulent structure of airflow within crop canopies. J. Meteorol. Soc. Japan Ser. II, 41, 317-326.

Inoue, K., Uchijima, Z., 1979. Experimental study of microstructure of wind turbulence in rice and maize canopy. Bull. Nat. Inst. Agr. Sci., Ser. A26, 1-88.

Jacquemin, B., Noilhan, J. 1990. Sensitivity study and validation of a land surface parameterization using the HAPEX-MOBILHY data set. Bound.-Layer Meteorol., 52, 93-134.

Kondo, J., Watanabe, T., 1992. Studies on the bulk transfer coefficients over a vegetated surface with a multilayer energy budget model. J. Atmos. Sci., 49, 2183-2199

Kondo, J., Saigusa, N., Sato, T., 1990. A parameterization of evaporation from bare soil surfaces. J. Appl. Meteorol., 385-389

Massman, W.J., Forthofer, J.M., Finney, A. 2017. An improved canopy wind model for predicting wind adjustment factors and wildland fire behavior. Can. J. For. Res., 47, 594-603, doi:10.1139/cjfr-2016-0354

McNaughton, K.G., 1983. The direct effect of shelter on evaporation rates: theory and an experimental test. Agri. Meteorol., 29, 125-136.

McNaughton, K.G., 1988. Effects of windbreaks on turbulent transport and microclimate. Agr. Ecosys. Environ., 22/23, 17-39.

Miller, D.R., Rosenberg, N.J., Bagley, W.T., 1973. Soybean water use in the shelter of a slat-fence windbreak. Agr. Meteorol., 11, 405-418.

Milly, P.C.D., 1986. An event-based simulation model of moisture and energy fluxes at a bare soil surface. Water Resour. Res., 22, 1680-1692.

Philip, J.R., 1957. The theory of infiltration, 4, Sorptivity and algebraic infiltration equations. Soil Sci., 84, 257-264.

Rosenberg, N.J., 1979. Windbreaks for reducing moisture stress, in: Barfield, B.J, Gerber, J.F. (Eds.), Modification of the Aerial Environment of Plants. ASAE, St Joseph, pp. 394-408.

Steven B. 1998. Windbreaks. Inkata Press, Port Melbourne.

Sugita, M., Matsuno, A., El-Kilani, R.M.M., Abdel-Fattah, A., Mahmoud, M.A., 2017. Crop evapotranspiration in the Nile Delta under different irrigation methods. Hydrol. Sci., J., 62. 1618-1635, doi: 10.1080/02626667.2017.1341631.

Toda, M., Sugita, M., 2003. Single level turbulence measurements to determine roughness parameters of complex terrain, J. Geophys. Res., 108, D12, 4363, doi: 10.1029/2002JD002573.

Tsuchihira, K., 2011. The estimation of evaporation and transpiration using hydrologic model in crop land of Nile Delta of Egypt. MS Thesis, Graduate School of Life and Environmental Science, University of Tsukuba. (in Japanese)

Uchijima, Z., 1976. Maize and rice, in Monteith, J.L., (ed.), Vegetation and the Atmosphere 2. Case Studies, Academic Press, pp.33-64.

Van Eimern, J., Karschon, R., Razumava, L.A., Robertson, G.W., 1964. Windbreaks and Shelterbelts. Technical Note No.59, WMO-No.147.TYP.70, Geneva, Switzerland, 188p.

Yi, C., 2008. Momentum transfer within canopies. J. Appl. Meteorol. Climatol. 47, 262–275, doi:10.1175/2007JAMC1667.1.

Table 1 Simulation run setting

Run	T_a	q_a	h_c	L_A	z_{0g}
R1	Measured values at Sakha-A		Measured values at Sakha-A (maize)		Determined for the furrow in Sakha-A (Table A.1)
R2	+5°C	×1. 05	NC	NC	×0.1
R3	NC	NC	×1/3	×0.5	NC

Note: R1 is the baseline case, and the variable(s) in other runs were varied in a relative sense against the run R1 settings. "NC" indicates no change, and the settings for run R1 were adopted without change.

Table A.1 List of parameters and functions adopted in the simulation

Category	Variable	Value(s)	Data Source/Reference
Canopy layer	$r_{st,\ \mathrm{min}}$ in Eq. (A.6)	57 s/m	Kubota (2014, personal comm.) and calibration (Sections A.1.1.1 and A3)
	$r_{st,\ \mathrm{max}}$ in Eq. (A.6)	6375 s/m	
	R_{gl} in Eq. (A.7)	100 W/m^2	Jacquemin and Noilhan (1990) and Uchijima (1976)
	a_2 and b_2 in Eq. (A.8)	a_2=0.09 and b_2=1	Kubota (2014, personal comm.) and Section A.1.1.1
	a_3 in Eq. (A.9)	0.0016	Jacquemin and Noihan (1990)
Soil layer	θ_s	0.63	Fujimaki and Hoshino
	θ_u	(assumed same as θ_s)	
	θ_w	0.25	
	θ_{fc}	0.47	
	K_s	6.6×10^{-7} m/s	

	z_{0g}	0.0286 m	Section A.1.1.1
	z_{0hg}	0.00121 m	
	a_1 and b_1 in Eq.(A.4)	a_1 =12 and b_1=10	Sections A.1.1.1 and A3
	H_b	0.5 m	
	A_0 in Eq. (A.23)	0.06201 (for z_{rz}<0.075 m) 0.08492 (for z_{rz}<0.175 m) 0.037827(for z_{rz}<0.375 m) 0.023313(for z_{rz}<0.775 m) 0.017851 (for z_{rz}>0.075 m) Unit: cm/s^2	Section A.1.2.2
	a_6 in Eq. (A.26)	0.25	

Figure caption

Fig. 1. (a) Relation between ΔE_c and ΔE for α = 0.1. For those points excluding points for $E_c = 0$ or $E_c \cong 0$ (identified as those after July 10), R^2 value is 0.83. (b) Same as (a) but for α = 0.9. For those points excluding points for $E_c = 0$ or $E_c \cong 0$ (identified as those after July 10), R^2 value is 0.85. (c) Relation between ΔE_c and ΔE_g for α = 0.1. (d) Same as (c) but for α = 0.9. (e) Relation between r_{c_PM} / r_{c_eq} and ΔE for α = 0.1. (f) Same as (e) but for α = 0.9.

Fig. 2. (a) Changes in relevant variables for the canopy layer when h_c was varied under otherwise the same meteorological condition observed in Aug.1 (experiment II).

Fig. 2. (b) Same as Fig.2. (a) but for the soil layer.

Fig. 2. (c) Changes in evapotranspiration when h_c was varied under the otherwise same meteorological condition observed in Aug.1.

Fig. 3. (a) Seasonal change in the simulated outputs of run R1 (experiment I) for $u = u_0$ and for $u = 0.1u_0$, together with some observed values.

Fig. 3. (b) Same as Fig.3. (a).

Fig. A.1. Comparison of E and E_g between measurements and estimated values after the calibration. The closed circles represent the comparison of E_g and open circles that of E.

Fig. A.2. Time series comparison of the simulated and measured variables for R_{lu}, E, and θ averaged in the root zone.

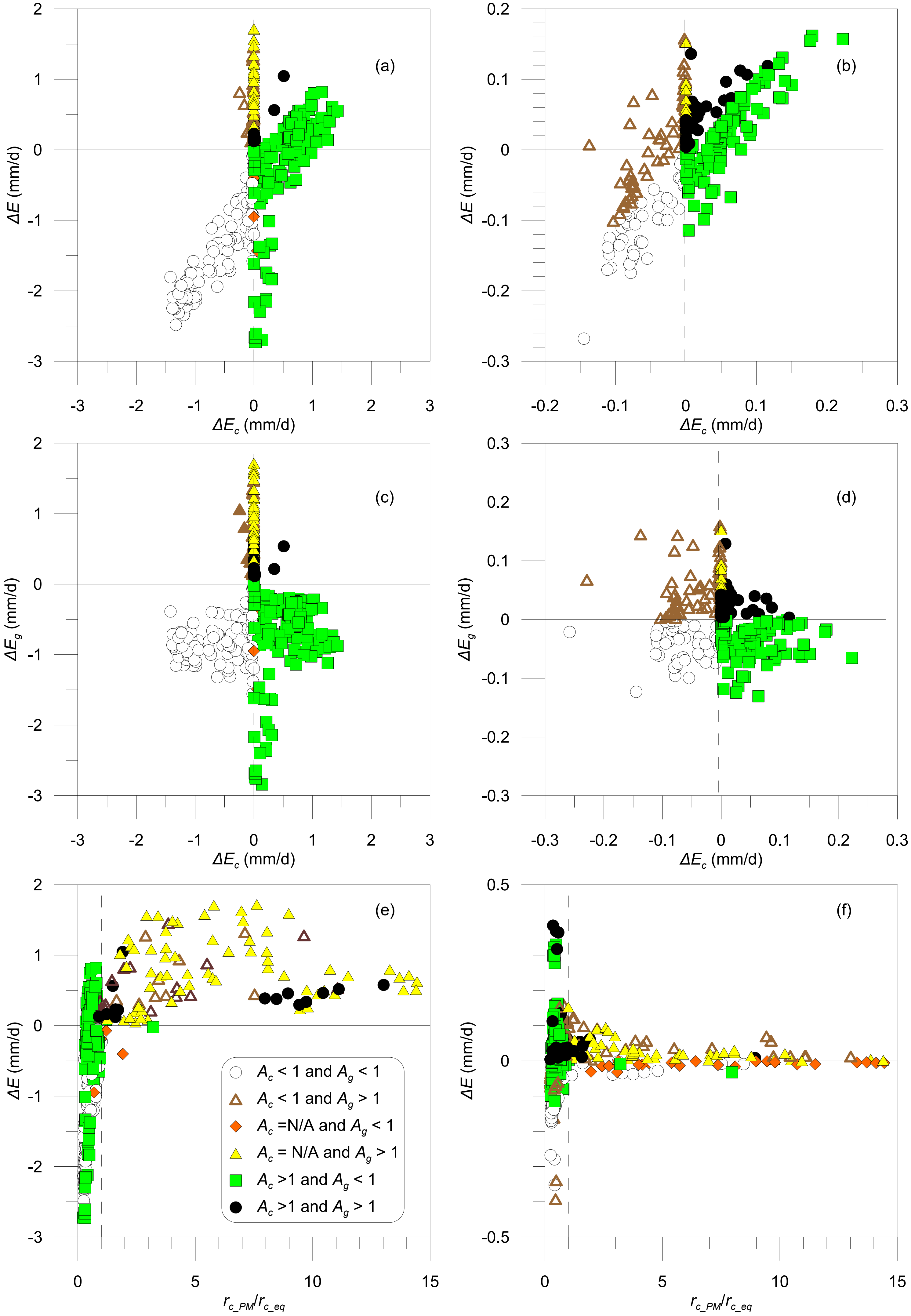

(a)
(b)
(c)
(d)
(e)
(f)
ΔE (mm/d)
ΔE_g (mm/d)
ΔE_c (mm/d)
r_c_PM/r_c_eq
A_c < 1 and A_g < 1
A_c < 1 and A_g > 1
A_c =N/A and A_g < 1
A_c = N/A and A_g > 1
A_c >1 and A_g < 1
A_c >1 and A_g > 1

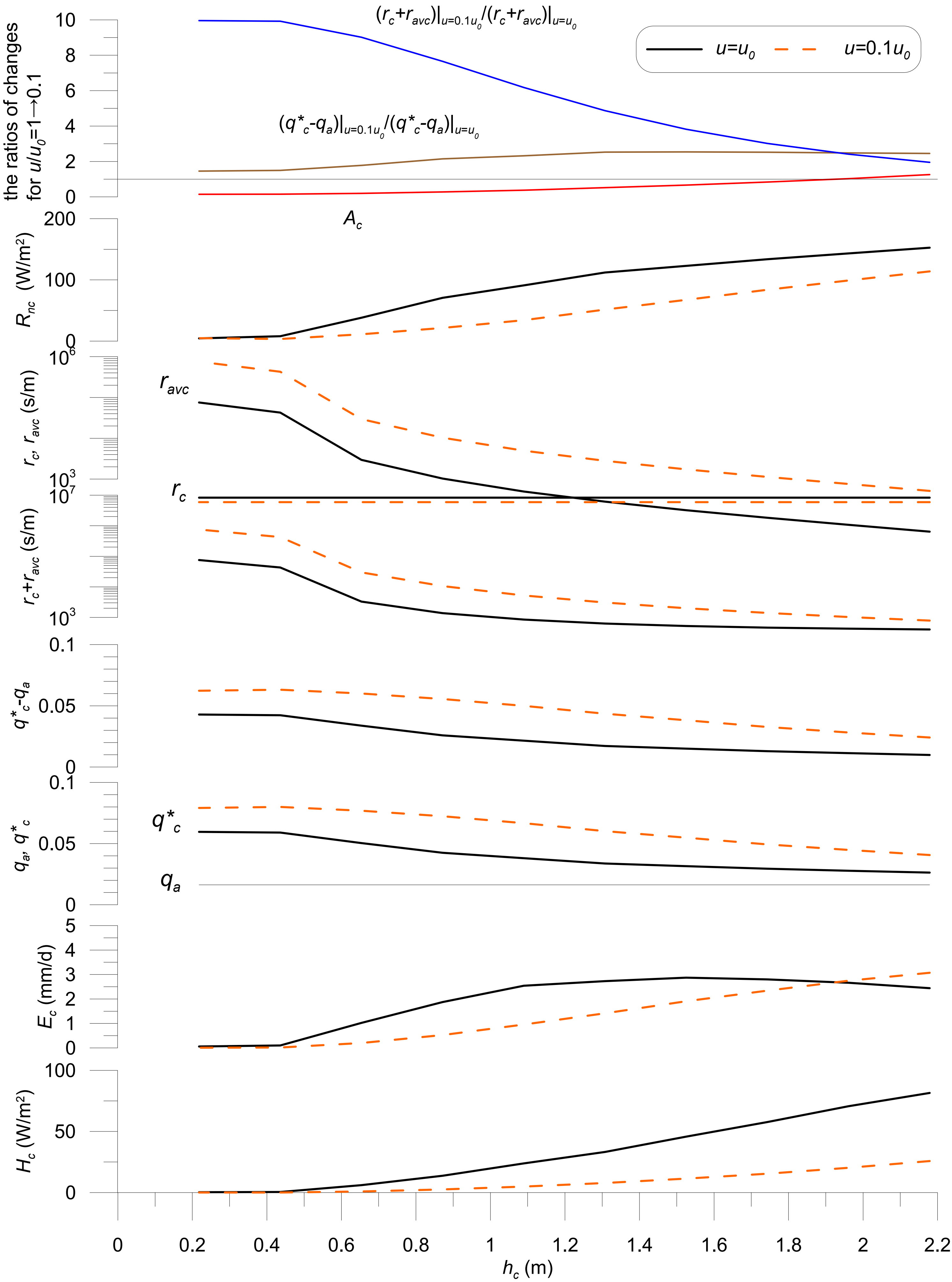

the ratios of changes for u/u_0=1→0.1
$(r_c+r_{avc})|_{u=0.1u_0}/(r_c+r_{avc})|_{u=u_0}$
$(q^*_c-q_a)|_{u=0.1u_0}/(q^*_c-q_a)|_{u=u_0}$
A_c
$u=u_0$
$u=0.1u_0$
R_{nc} (W/m²)
r_c, r_{avc} (s/m)
r_{avc}
r_c
r_c+r_{avc} (s/m)
$q^*_c-q_a$
q_a, q^*_c
q^*_c
q_a
E_c (mm/d)
H_c (W/m²)
h_c (m)

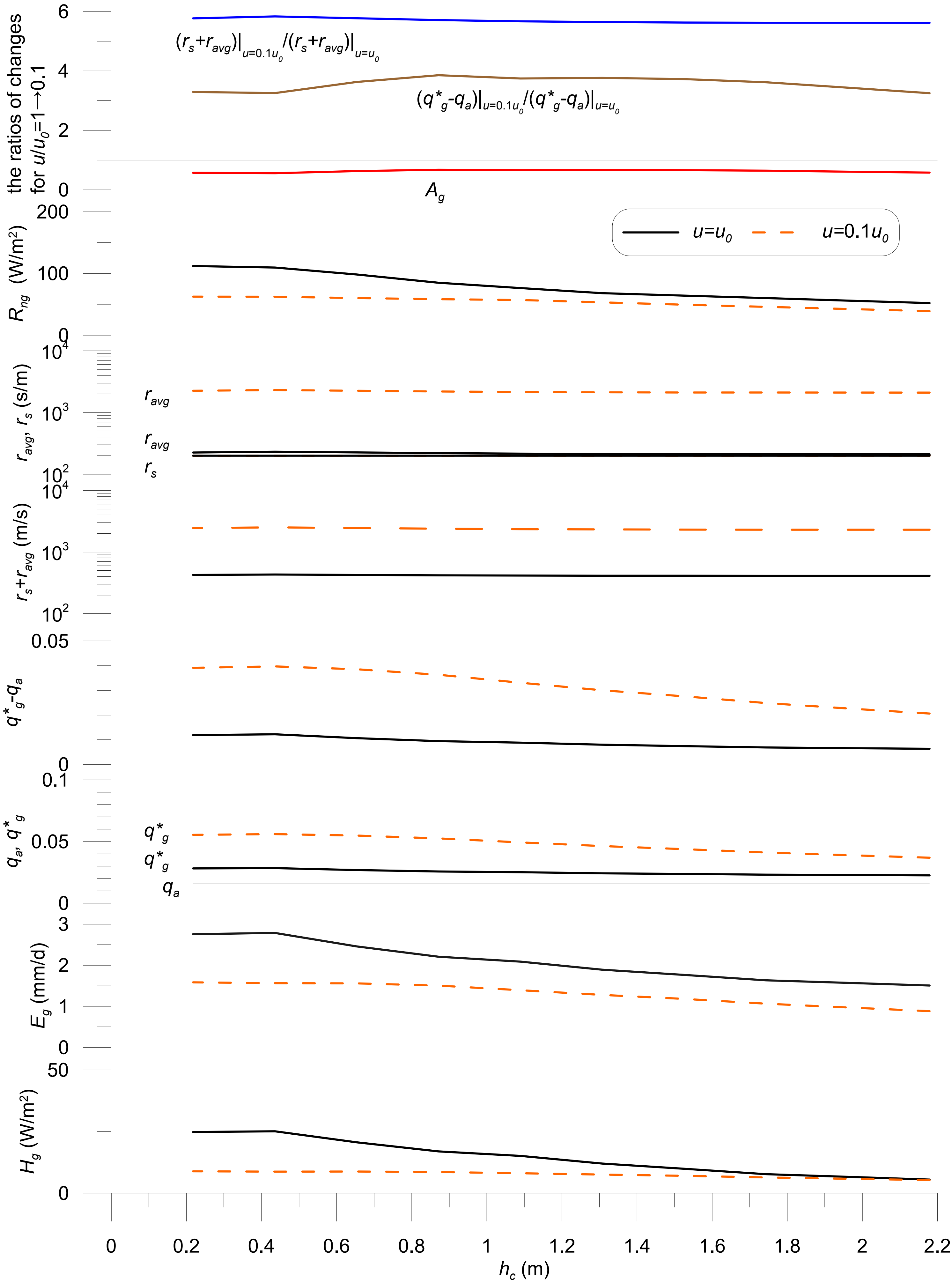

the ratios of changes for u/u0=1→0.1
(rs+ravg)|u=0.1u0/(rs+ravg)|u=u0
(q*g-qa)|u=0.1u0/(q*g-qa)|u=u0
Ag
u=u0
u=0.1u0
Rng (W/m2)
ravg, rs (s/m)
ravg
ravg
rs
rs+ravg (m/s)
q*g-qa
qa, q*g
q*g
q*g
qa
Eg (mm/d)
Hg (W/m2)
hc (m)

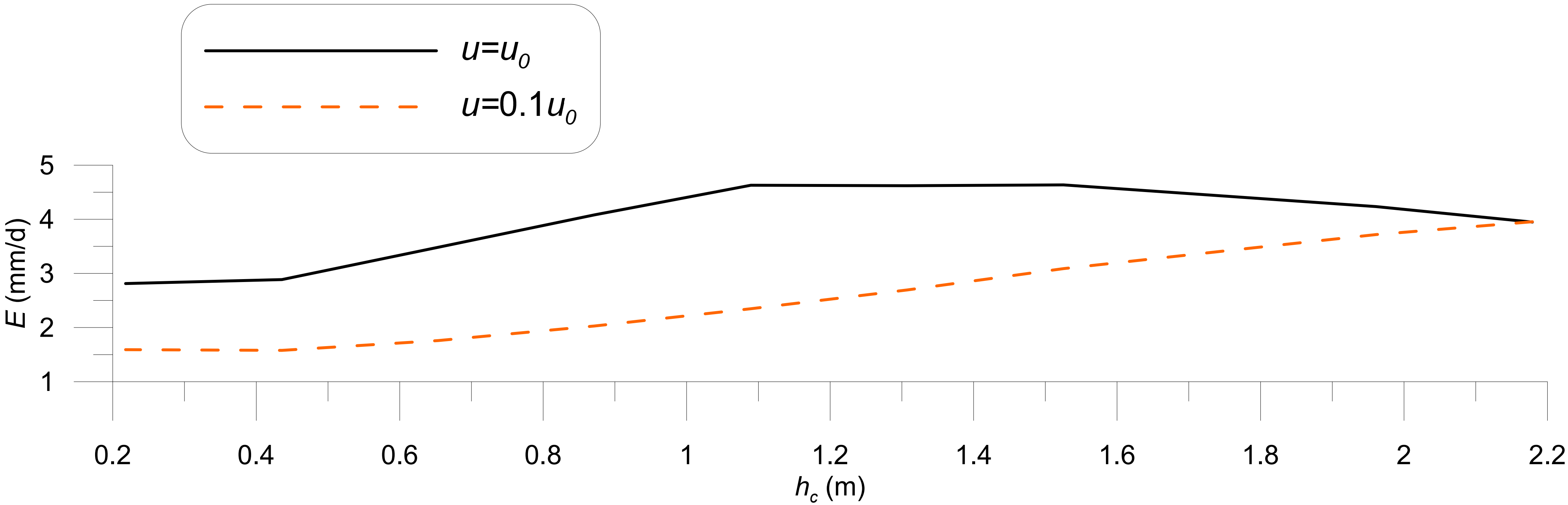

u=u0
u=0.1u0
5
4
3
2
1
E (mm/d)
0.2
0.4
0.6
0.8
1
1.2
1.4
1.6
1.8
2
2.2
hc (m)

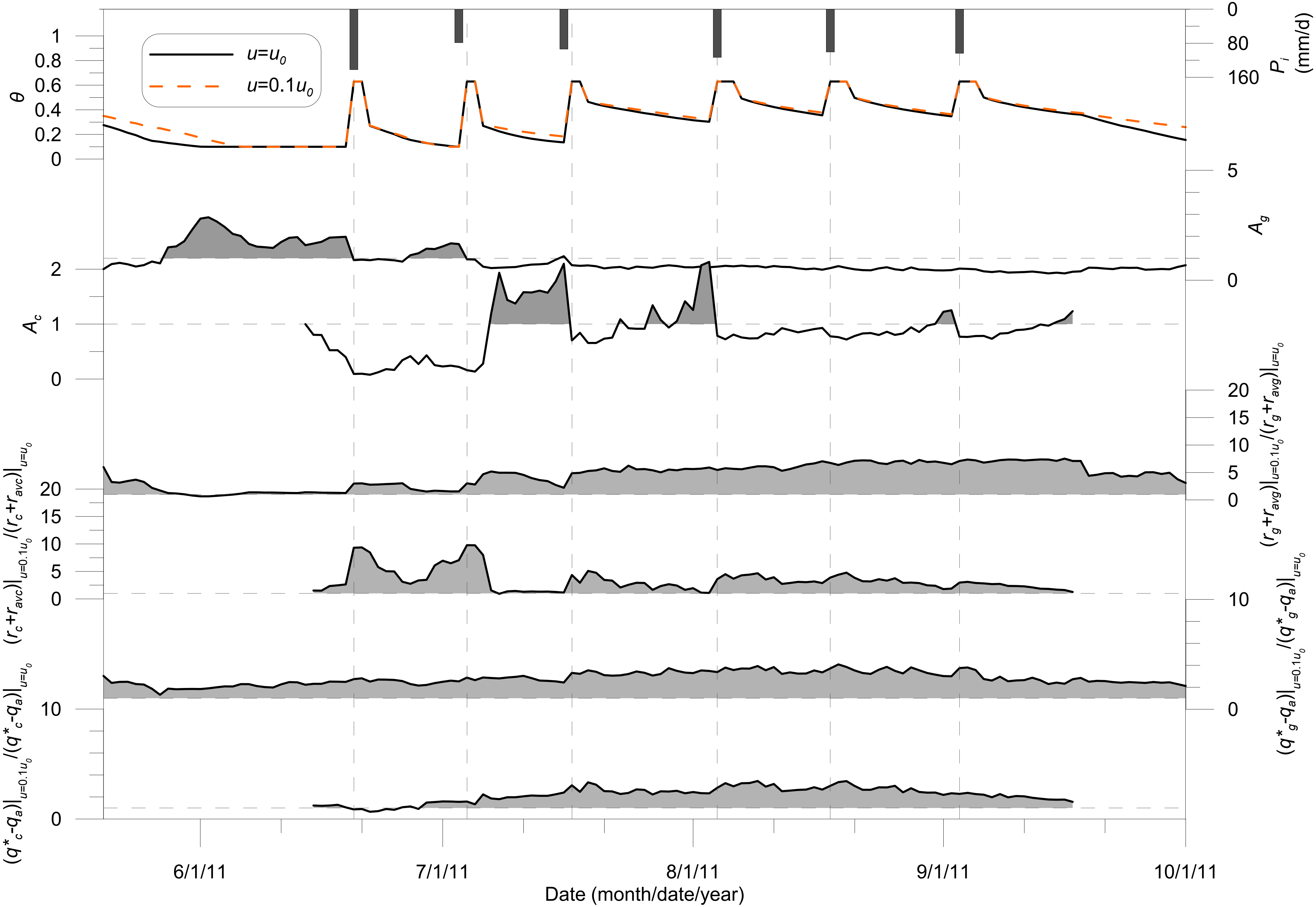

u=u0
u=0.1u0
θ
Pi (mm/d)
0
80
160
1
0.8
0.6
0.4
0.2
0
5
Ag
0
2
Ac
1
0
20
15
10
5
0
(rg+ravg)|u=0.1u0/(rg+ravg)|u=u0
20
15
10
5
0
(rc+ravc)|u=0.1u0/(rc+ravc)|u=u0
10
0
(q*g-qa)|u=0.1u0/(q*g-qa)|u=u0
10
0
(q*c-qa)|u=0.1u0/(q*c-qa)|u=u0
6/1/11
7/1/11
8/1/11
9/1/11
10/1/11
Date (month/date/year)

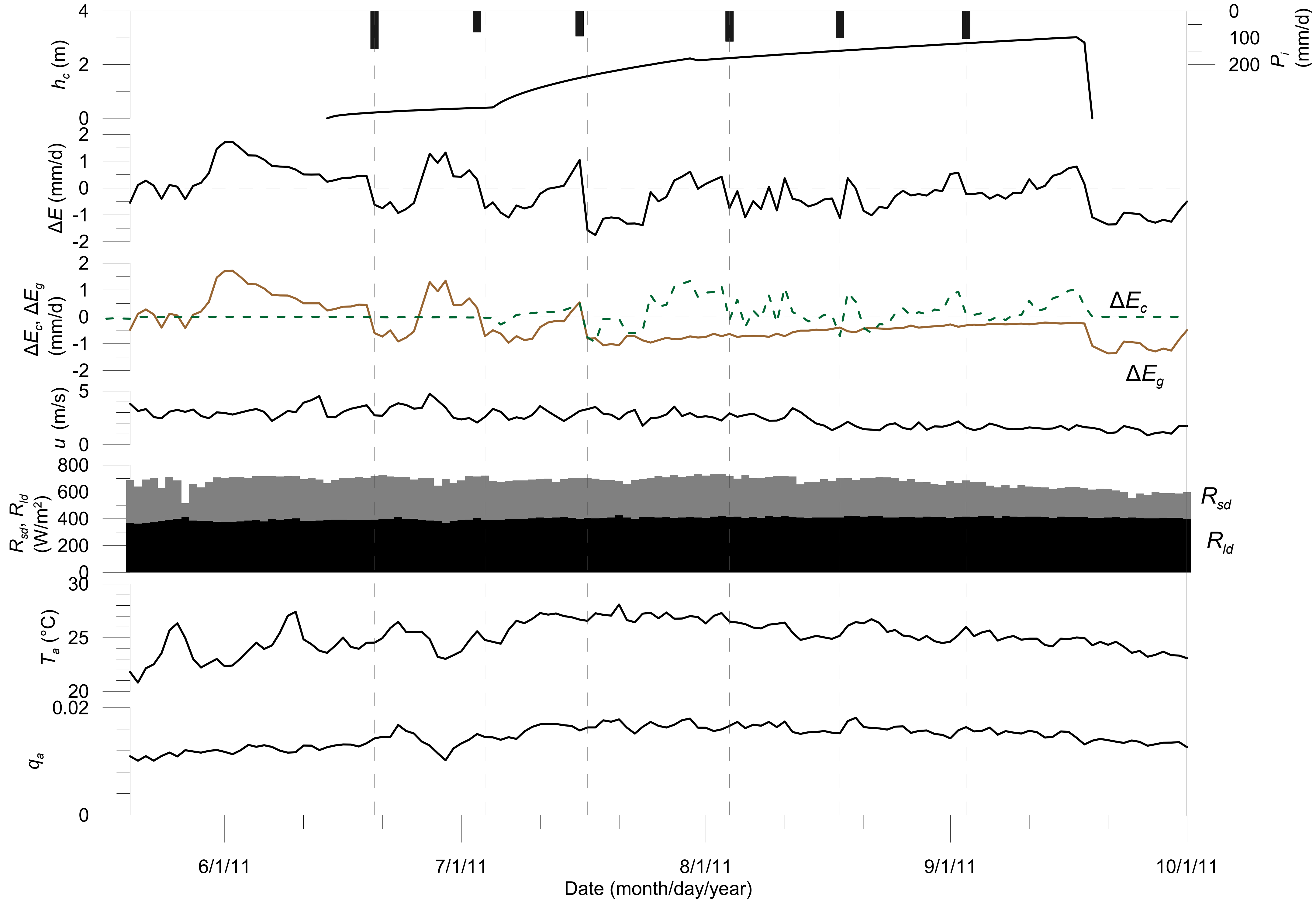

4
2
0
h_c (m)
0
100
200
P_i (mm/d)
2
1
0
-1
-2
ΔE (mm/d)
2
1
0
-1
-2
ΔE_c, ΔE_g (mm/d)
ΔE_c
ΔE_g
5
0
u (m/s)
800
600
400
200
0
R_{sd}, R_{ld} (W/m^2)
R_{sd}
R_{ld}
30
25
20
T_a (°C)
0.02
0
q_a
6/1/11
7/1/11
8/1/11
9/1/11
10/1/11
Date (month/day/year)

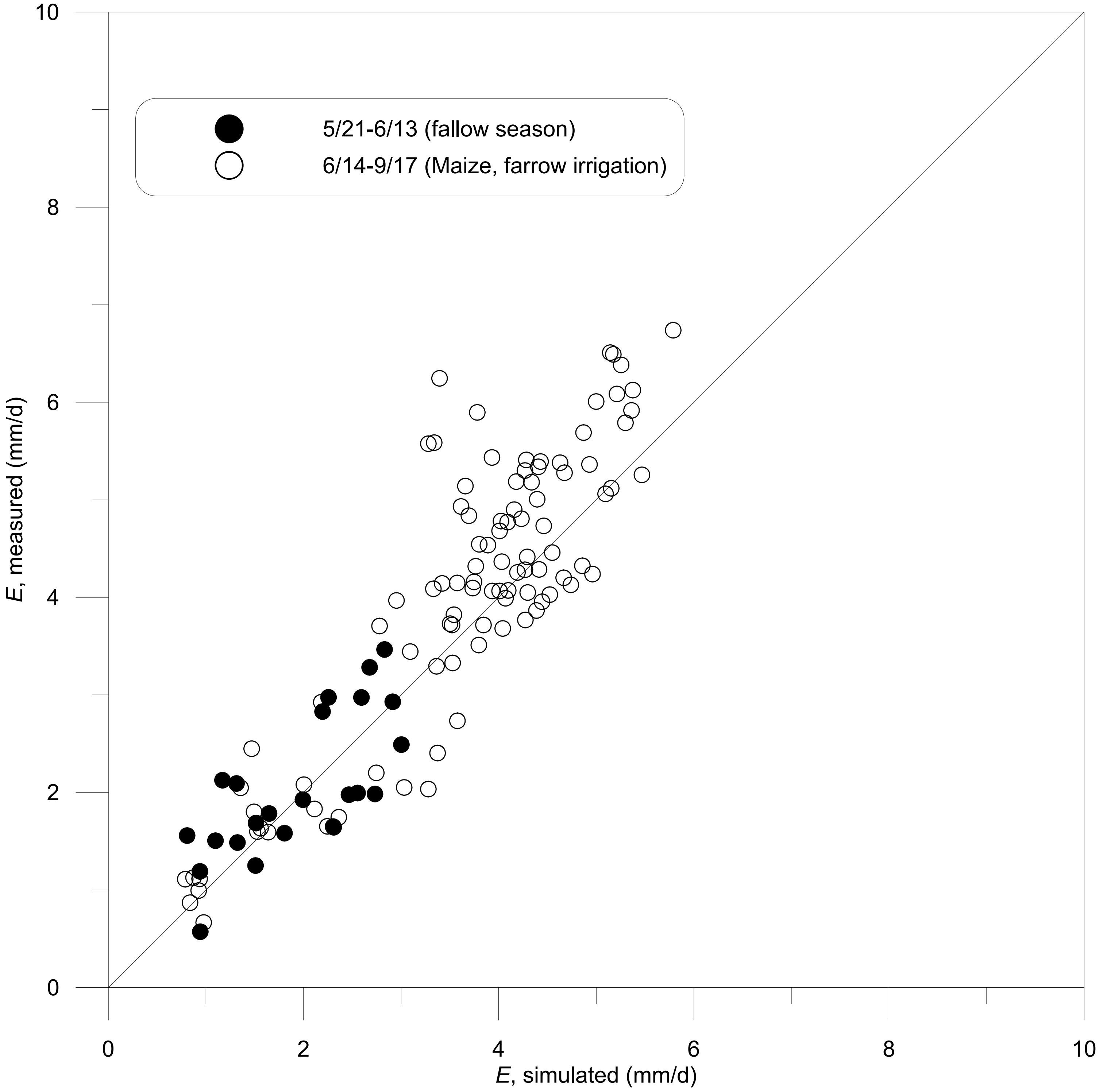
10
8
6
4
2
0
0
2
4
6
8
10
E, measured (mm/d)
E, simulated (mm/d)
5/21-6/13 (fallow season)
6/14-9/17 (Maize, farrow irrigation)

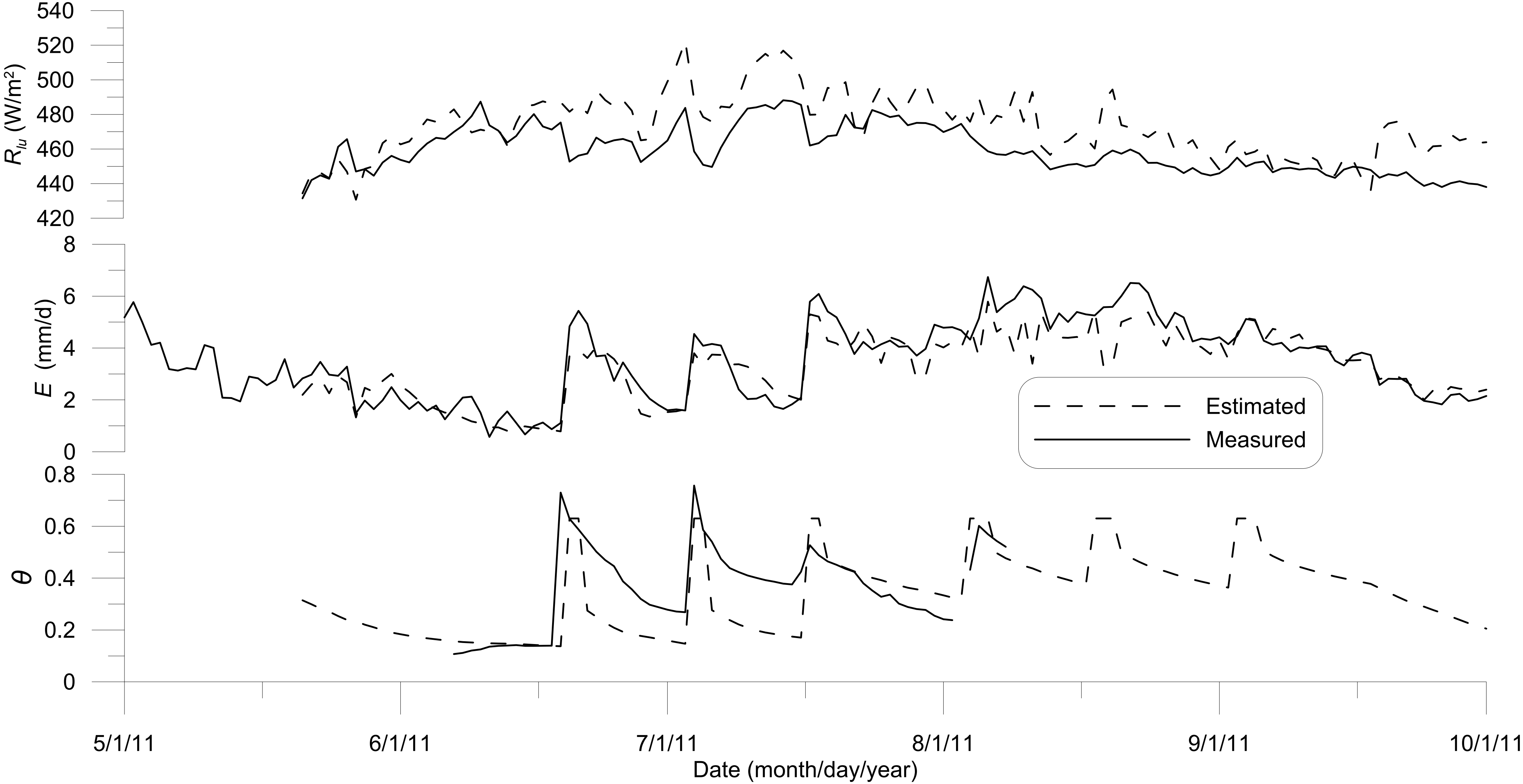

540
520
500
480
460
440
420
R_{lu} (W/m^2)
8
6
4
2
0
E (mm/d)
Estimated
Measured
0.8
0.6
0.4
0.2
0
θ
5/1/11
6/1/11
7/1/11
8/1/11
9/1/11
10/1/11
Date (month/day/year)